Conductive Three-Dimensional Material Assembled from Silver Nanoparticles Using a Conjugated Dithiol Linker

Cuijie Jiang, David John Cardin,* and Shik Chi Tsang

Department of Chemistry, The University of Reading, Whiteknights, Reading, Berkshire RG6 6AD, U.K.

Received July 27, 2007
Revised Manuscript Received October 16, 2007

In the last ten years there has been rapidly growing interest in the development of functional nanomaterials.[1] One strategy is to assemble such particles or hybrid networks from their basic building blocks. The variety of such building blocks available (nature, structure, size, and functionality) and of potential linkers allows assembly of an extensive range of different architectures and organic–inorganic interfaces, resulting from different assembly strategies.[2] One recent notable success has been the development of polymeric chains of nanoparticles utilizing the singularities present as a result of the "hairy ball" theorem.[3] Structures such as these have potential as electro-photonic band gap materials, and assemblies using more than one type of nanoparticle have potential as supercapacitors or as catalysts.

We now report a regular, three-dimensional conductive nanoparticle network constructed by linking the particles via a conjugated organic dithiol, and analogous nonconducting assemblies linked through nonconjugated organic dithiols. The regularity is established by X-ray diffraction (XRD) data (see below) though the more selective transmission electron microscopy (TEM) technique shows areas of variable regularity. Such conducting assemblies open up exciting possibilities for optical and electronic properties. It is noteworthy that a two-dimensional superlattice of gold nanoparticles linked through organic molecules was reported in 1996,[4] and the electronic properties of similar monolayers have been extensively studied since that time. However, no three-dimensional network of silver nanoparticles has been obtained.

Dodecanethiol-capped silver nanoparticles were prepared following Brust et al.'s method.[5] Aqueous silver nitrate (20 mL, 50 mM) was added to a solution of tetra-*n*-octylammonium bromide (80 mL, 4 mM) in toluene. The two-phase mixture was vigorously stirred (1 h) until the silver had been completely transferred into the organic phase. 1-Dodecanethiol (0.2 g, 1 mmol) was added and the mixture stirred (20 min). Fresh aqueous sodium borohydride (10 mL, 1 M) was introduced as reductant and the mixture stirred vigorously overnight. The aqueous layer was removed, the organic phase reduced under vacuum (to ca. 5 mL), and ethanol (200 mL) added to the concentrated toluene solution, causing precipitation. The precipitate was removed by filtration, redissolved in toluene, and reprecipitated several times to purify, finally affording precipitate 1. A toluene solution of this material was mixed with an excess of the appropriate dithiol (1,4-benzenedithiol, 1,4-butanedithiol, or 1,9-nonanedithiol) resulting in precipitation after several hours. Changes during this reaction were monitored by ^{1}H NMR spectroscopy, using signals of the thiols. The final product was filtered off, washed twice with ethanol, dried, and stored under vacuum as precipitate 2. Conductivity measurements were made using a two-probe electrode system, on samples of both precipitate 1 and precipitate 2 which had been pressed into circular pellets (13 mm diameter by 200–450 μm) with a 10-ton press.

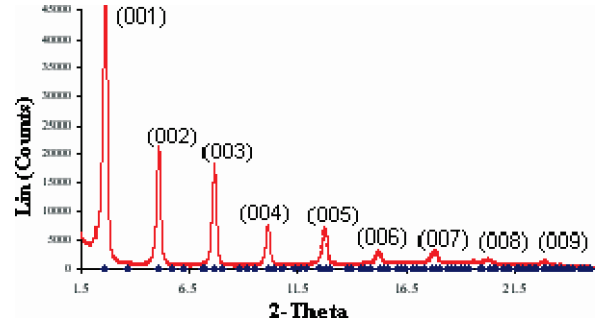

Figure 1. Small angle XRD of precipitate 1.

XRD of precipitate 1 confirms the presence of the silver metal phase ($2\theta = 38.25°$) corresponding to the κ plane (see also Supporting Information). The small-angle region clearly shows the formation of a regular superlattice, reflecting an efficient self-assembly in the solid-state, Figure 1. As can be seen from the figure, the strong sharp peaks can be indexed as a primitive cubic structure with unit cell a = 34.96(2) Å (refined by CHECK CELL[6]) with a best fit of 0.0066.

Figure 2a shows a TEM micrograph of precipitate 1, for Ag-$SC_{12}H_{25}$ particles, showing the highly monodisperse nature and good ordering of the sample. Most of the material lies in the size range 3–4 nm (for full details see the Supporting Information) and is in excellent agreement with the unit cell length determined from the low-angle XRD data, indicating a close-packed structure in the solid state.

The NMR data (see Supporting Information for spectra) reveal how the added dithiol species displace the initially

* Corresponding author. E-mail: d.j.cardin@reading.ac.uk.

(1) (a) Okamura, M.; Kondo, T.; Uosaki, K. *J. Phys. Chem. B* **2005**, *109*, 9897–9904. (b) Cliffel, D. E.; Zamborini, F. P.; Gross, S. M.; Murray, R. W. *Langmuir* **2000**, *16*, 9699–9702. (c) Brust, M.; Fink, J.; Bethell, B.; Schiffrin, D. J.; Kiely, C. *Chem. Commun.* **1995**, 1655–1656.
(2) (a) Zhang, X.; Li, D.; Zhou, X. P. *New J. Chem.* **2006**, *30*, 706–711. (b) Itoh, H.; Tahara, A.; Naka, K.; Chujo, Y. *Langmuir* **2004**, *20*, 1972–1976. (c) Bönnemann, H.; Waldöfner, N.; Haubold, H. G.; Vad, T. *Chem. Mater.* **2002**, *14*, 1115–1120.
(3) DeVries, G. A.; Brunnbauer, M.; Hu, Y.; Jackson, A. M.; Long, B.; Neltner, B. T.; Uzun, O.; Wunsch, B. H.; Stellacci, F. *Science* **2007**, *315*, 358–361.
(4) Andres, R. P.; Bielefeld, J. D.; Henderson, J. L.; Janes, D. B.; Kolagunta, V. R.; Kubiak, C. P.; Mahoney, W. J.; Osichin, R. G. *Science* **1996**, *273*, 1690–1693.
(5) Brust, M.; Walker, M.; Bethell, D.; Schiffrin, D. J.; Whyman, R. *Chem. Commun.* **1994**, 801–802.
(6) Iaugier, J.; Bochu, B. *LMGP suite of programmes for the interpretation of X-ray experiments*; ENSP/Laboratoire des Matériaux et du Génie Physique: SaintMartin d'Hères, France, 2000.

10.1021/cm7020615 CCC: $40.75
Published on Web 12/06/2007

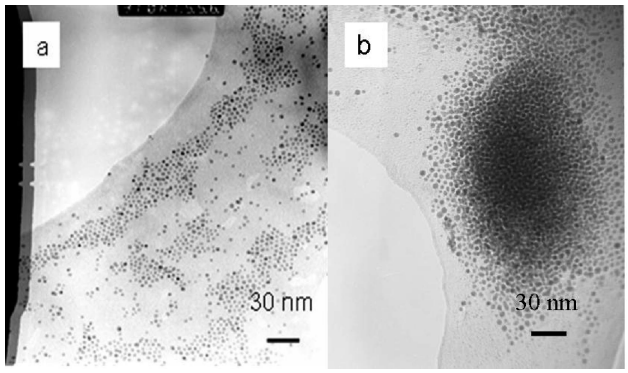

Figure 2. (a) TEM of precipitate 1; (b) TEM of precipitate 2.

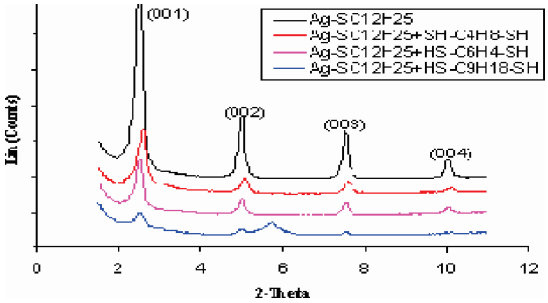

Figure 3. (Small angle) XRD patterns of precipitate 1 (top curve) compared with those of precipitate 2 for 1,4-butanedithiol, (second curve down) 1,4-benzenedithiol, (third curve), or 1,9-nonanedithiol (lowest curve).

coordinated monothiols and release them into solution. In the spectrum of nanoparticles stabilized by dodecanethiol, the ligand peaks are both weak and broad, presumably owing to slow rotation of the large particles in solution. When 1,4-benzenedithiol is added to this solution initially the spectrum is essentially a superimposition of the particle spectrum plus that of the added dithiol. After 5 h, the spectrum shows release of free dodecanethiol and a marked decrease in the intensity of both the aromatic and thiol protons from the added dithiol. Figure 2b shows a TEM of precipitate 2, for the case of displacement by 1,4-benzenedithiol, and reveals the close aggregation of the primary particles. Furthermore, these aggregates are sulfur-rich, as unambiguously shown by energy-dispersive X-ray measurements, owing to the presence of the dithiol linkers.

Comparison of the XRD data for precipitate 1 with those for precipitate 2 (for all three linkers, see Figure 3) shows that in each case they are similar, reflecting similar lattice parameters for the three networks. For the case of 1,9-nonanedithiol, however, there is an additional small peak, which probably arises from the presence of a minor impurity. Thus, the XRD data reveal that the regular packing of the particles is not greatly affected by the nature or length of the linkers and appears to be determined largely by the much larger particles (compared to the linkers) which are approximately close-packed with the nonrigid thiol molecules wrapped partially around in a thin corona-like layer. Similar packing of dodecanethiol-stabilized silver nanoparticles was observed by Fitzmaurice and co-workers.[7] The TEM of precipitate 2 shows regular ordering which is clearly visible

(7) Korgel, B. A.; Fullam, S.; Connolly, S.; Fitzmaurice, D. *J. Phys. Chem. B* **1998**, *102*, 8379–8388.

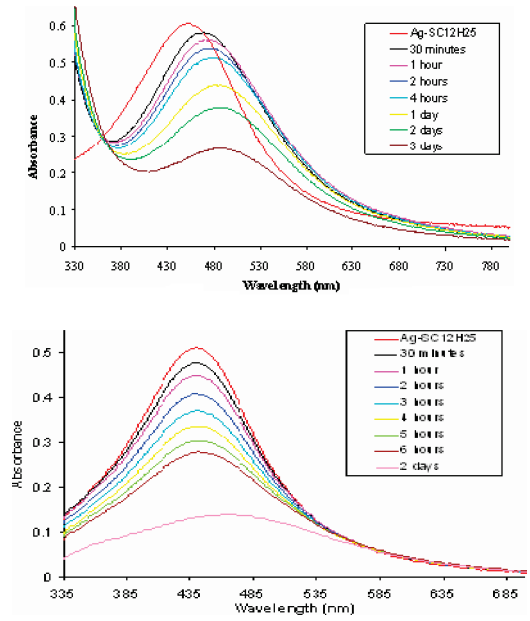

Figure 4. Time-evolved UV–visible spectra of the Ag-$SC_{12}H_{25}$ nanoparticle in toluene when mixed with 1,4-benzenedithiol (top) and 1,9-nonanedithiol (bottom). Time increases from top to bottom in both figures.

around the edges of the dark area and also the three-dimensional nature of the network. This ordering is supported by the XRD data; see Figure 3.

UV–vis spectra for the nanoparticles were recorded in toluene solution and are reproduced in Figure 4. The surface plasmon (SP) peak for the silver nanoparticles is clearly visible at approximately 440 nm. This peak shifts significantly to longer wavelength (ca. 475 nm) on addition of 1,4-benzenedithiol, but no analogous shift in the SP peak was observd on addition of 1,9-nonanedithiol. These observations can be correlated with the conjugated nature of the benzenedithiol linker, compared with the saturated linker, and with electronic communication between particles linked by the conjugated species. It is well-established that silver (and certain other noble metal) nanoparticles have defined SP frequencies which depend on the size (and shape) of the particle. Thus the change in SP frequency on addition of the 1,4-benzenedithiol can be traced to a change in the effective size of the particles, resulting from an electronic communication through this conjugated linker. The lack of change in SP frequency on addition of 1,9-nonanedithiol suggests no change on the effective particle size or, correspondingly, no electronic communication between particles linked by the saturated bridge.

These observations in SP effects prompted us to study the electronic conductivity of our networks. Table 1 shows how the conductivity of the silver nanoparticle network formed with the conjugated 1,4-benzenedithiol linker is 5 orders of magnitude higher than that of networks formed from the nonconjugated linkers. This is in harmony both with expectations relating to electronic transmission through conjugated versus nonconjugated systems, but also in agreement with the red-shift in the SP frequency of the network formed using the conjugated linker. Such conduction has been modeled in detail for gold-linker-gold assemblies by Ning and co-

Table 1. Conductance of Precipitate 1 and Precipitate 2 (1,4-Benzenedithiol, 1,4-Butanedithiol, or 1,9-Nonanedithiol)

material	conductance (S cm^{-1})
Ag-$SC_{12}H_{25}$ nanoparticle	1.74×10^{-10}
Ag nanonetwork formed by chemical exchange between Ag-$SC_{12}H_{25}$ nanoparticle and 1,4-benzenedithiol	2.02×10^{-5}
Ag nanonetwork formed by chemical exchange between Ag-$SC_{12}H_{25}$ nanoparticle and 1,4-butanedithiol	6.00×10^{-10}
Ag nanonetwork formed by chemical exchange between Ag-$SC_{12}H_{25}$ nanoparticle and 1,9-nonanedithiol	3.64×10^{-10}

workers.[8] They used a Green's function approach coupled with hybrid tight-binding DFT methods to calculate the conductance of such systems. The problem of estimating the energy difference between the Fermi energy and the HOMO was overcome using UV−photoelectron spectroscopic data. Furthermore, for the molecular junctions, a density of states approach was used taking gold clusters as the model, which should compare well with our nanoparticles. No calculations at this level appear to have been carried out for silver junctions, but given the similar values of the (bulk) resistivities, for the present purposes, this should have only a minor effect. The findings, which qualitatively agree well with experiment overall and nearly quantitatively for the benzenedithiol linker, show that the conductance varies little with geometry at the junction and is greater for conjugated systems than for saturated systems (as we find experimentally). The decrease in conductance on going from a conjugated to a saturated linker is calculated to be 3 orders of magnitude using a C_{10} linker. Given the uncertainty in our contacts both to the nanoparticle and of the nanoparticle with the measuring electrode, the results agree as well as could be expected with our measurements using a C_9 linker.

We have thus demonstrated the first preparation of a three-dimensional nanoparticle network of silver particles, linked through dithiol bridges, and how the electrical conductivity and SP resonance frequency can be related to the nature of the linkers employed.

Supporting Information Available: Figure S1, a typical XRD of Ag-$SC_{12}H_{25}$ nanoparticle (Precipitate 1); Figure S2, the size distribution of Ag-$SC_{12}H_{25}$ nanoparticles derived from TEM; Figure S3, time-evolved ^{1}H NMR spectra of Ag-$SC_{12}H_{25}$ nanoparticles in solution when mixed with 1,4-benzenedithiol (PDF). This material is available free of charge via the Internet at http://pubs.acs.org.

CM7020615

(8) Ning, Z.; Chen, J.; Hou, S.; Zhang, J.; Liang, Z.; Zhang, J.; Han, R. *Phys. Rev. B* **2005**, *72*, 155403–1–7.